

The NIR to UV continuum of radio loud vs. radio quiet quasars

M. Labita^{1*}, A. Treves¹ and R. Falomo²

¹*Department of Physics and Mathematics, University of Insubria, Via Valleggio 11, I-22100 Como, Italy*

²*INAF, Astronomical Observatory of Padova, Vicolo dell'Osservatorio 5, I-35122 Padova, Italy*

Accepted ... Received ...; in original form ...

ABSTRACT

Starting from a sample of SDSS quasars appearing also in the 2MASS survey, we study the continuum properties of ~ 1000 objects observed in 8 bands, from NIR to UV. We construct the mean spectral energy distribution (SED) and compare and contrast the continua of radio loud (RLQ) and radio quiet (RQQ) objects. The SEDs of the two populations are significantly different, in the sense that RLQs are redder with power law spectral indices $\langle\alpha_{\text{RLQ}}\rangle = -0.55 \pm 0.04$ and $\langle\alpha_{\text{RQQ}}\rangle = -0.31 \pm 0.01$ in the spectral range between $10^{14.5}$ and $10^{15.35}$ Hz. This difference is discussed in terms of different extinctions, different disc temperatures, or slopes of the non-thermal component.

Key words: galaxies: active – galaxies: nuclei – quasars: general.

1 INTRODUCTION

A substantial effort has been dedicated to construct the spectral energy distributions (SEDs) for sizeable samples of quasars over the whole accessible range of the electromagnetic spectrum (see e.g. Sanders et al. 1989; Francis et al. 1991; Elvis et al. 1994; Richards et al. 2006). However, only a few papers focus on the comparison between the SEDs of radio loud (RLQ) and radio quiet (RQQ) quasars. Elvis et al. 1994 propose an overall spectrum from a sample of 47 quasars, divided in RLQs and RQQs, which shows that no distinction between the SEDs of the two subsamples is apparent in the range $100\mu\text{--}1000\text{\AA}$. As noted by these authors, the considered sample is biased towards X-ray and optically bright quasars. Some indication of a possible difference between the NIR to optical colors of RLQs and RQQs in the 2MASS catalogue was reported by Barkhouse & Hall (2001). Francis, Whiting & Webster (2000) found that the optical–NIR continuum is significantly redder in radio selected RLQs from the PKS Half-Jansky Flat-Spectrum survey than in optically selected RQQs from the Large Bright Quasar Survey (LBQS). These and other works (e.g. Kotilainen et al. 2007) indicate that radio loud objects are possibly redder than their radio quiet counterparts, but the samples seriously suffer of selection effects against red radio quiet quasar, because RQQs are mostly collected from optical selected samples (e.g. the LBQS, the first selection criterion of which is “blue color” of candidates; see Hooper, Impey & Foltz 1997). White et al. suggest that redder quasars from the Sloan Digital Sky Survey (SDSS) are likely to be more radio-powerful

than bluer objects, and this is an indication that the red color of radio loud objects is not completely due to the bias against red RQQs in optically selected samples, since the two classes of objects derive from the same survey.

Because of the importance of the distinction between RLQs and RQQs in the Unified Models of AGN, these results suggest and motivate a study aimed at investigating the properties of the continuum emission of quasars in the UV to NIR region, in order to compare and contrast the SEDs of radio loud and radio quiet objects.

In Section 2 we focus on the quasar sample selection criteria and on the host galaxy contribution. In section 3 we consider the SED construction and discuss the spectral shape. The RLQ and RQQ SEDs are then compared and contrasted. In the last section we provide a summary and a discussion of the results.

Throughout this paper, we adopt a concordant cosmology with $H_0 = 70 \text{ km s}^{-1} \text{ Mpc}^{-1}$, $\Omega_m = 0.3$ and $\Omega_\Lambda = 0.7$.

2 SAMPLE SELECTION

In order to mark similarities and differences of the continuum spectroscopic properties of RLQs and RQQs, our first aim is the selection of a quasar sample which is minimally biased against the radio properties and the nuclear color of the objects. We start our analysis from the Sloan Digital Sky Survey (SDSS) quasar catalogue III (Schneider et al. 2005); we then require that objects are in the observation area of the Faint Images of the Radio Sky at Twenty-cm (FIRST, Becker et al. 2003), which is the reference catalogue for radio data, in order to allow the distinction between RLQs

* E-mail: marzia.labita@uninsubria.it

and RQQs. Finally, this sample is cross-correlated with the Two Micron All Sky Survey (2MASS, Cutri et al. 2003) in order to have detections in the near-infrared (NIR) bands.

2.1 SDSS quasar catalogue

The SDSS quasar catalogue (46420 objects) covers about 4188 deg² and selects objects that have luminosities larger than $M_i = -22$, have at least one emission line with FWHM larger than 1000 km/s or are unambiguously broad absorption line objects, are fainter than $i = 15.0$ and have highly reliable redshifts.

Note that the SDSS quasar catalogue suffers from a small bias in favour of radio loud objects, as a FIRST detection is one of the starting criteria to select quasar candidates; anyway White et al. (2007) verified that this introduces at most a very minor bias towards higher radio-optical ratios.

2.2 FIRST: distinction between RLQs and RQQs

Starting from the SDSS quasars, we focus on those which are in the FIRST observation area, but we don't exclude *a priori* the objects which are under the FIRST flux limit (1 mJy), so that no bias against the radio power is introduced.

The distinction between radio loud and radio quiet objects is usually made referring to the ratio between the radio and optical flux. Here we assume that a QSO is radio loud if:

$$R_{r-o} = \frac{F_\nu(1.5 \cdot 10^9 \text{Hz})}{F_\nu(6 \cdot 10^{14} \text{Hz})} > 10 \quad (1)$$

and radio quiet otherwise¹ (e.g. Kellermann et al. 1989). Note that our division between RLQs and RQQs should not be considered a physical bimodality, an issue on which there is still controversy in the literature (e.g. Goldschmidt et al. 1999; Ivezić et al. 2002; Jiang et al. 2007). Yet our division is a simple separation in two groups of high or low radio power with respect to a certain limit. We verified that all the results presented here remain substantially unchanged adopting different limits (5 or 30) for the distinction between RL and RQ objects.

There are not radio data for all the objects in the sample (91% of the objects are below the FIRST radio flux limit), and obviously the larger part of these are expected to be radio quiet objects. In order not to introduce a bias against the ratio of RLQs and RQQs, we select all the objects which have $g < 18.9$, so that for this subsample we can discriminate between RLQs and RQQs. In fact, if an object has a radio flux under the FIRST limit (i.e. $F_\nu(1.5 \cdot 10^9 \text{Hz}) < 1 \text{mJy}$) and $g < 18.9$ (i.e. $F_\nu(6 \cdot 10^{14} \text{Hz}) > 0.1 \text{mJy}$), because of condition (1) it is a RQQ, while we could not discriminate if $g > 18.9$. This restriction reduces the sample by 66%, keeping the original ratio between the number of RQQs and RLQs. We obtain a sample of 14395 objects, 1105 of which are RLQs and 13290 are RQQs. From the SLOAN data, we derived the u , g , r , i , z magnitudes. The values were

corrected for Galactic extinction, following the indications given in Schneider et al. (2005).

2.3 NIR detections from 2MASS

The SLOAN-FIRST sample was then cross-correlated with the 2MASS catalogue, in order to obtain the J , H and K magnitudes of the objects. The 2MASS survey is a collection of near-infrared uniformly-calibrated observations of the entire sky; sources brighter than about 1 mJy in each band were detected with a signal-to-noise ratio greater than 10. The cross-correlation strongly reduces the sample, which now consists of 1761 common objects with observations in 8 bands each. We assumed two objects are matched if their separation angle is less than 0.2 arcsec, which roughly corresponds to the position error of the catalogues². Obviously the request of a 2MASS detection introduces a bias in the sample, as among high redshift (low luminosity) objects the redder ones are more likely detected. In the following we will come back on this issue.

2.4 Host galaxy component

A host galaxy component could affect the luminosity measures in part of the selected quasars. We require that the selected objects to have a negligible galaxy component with respect to the nuclear flux. Assuming that all the galaxies are ellipticals (SED from Mannucci et al. 2001), purely passively evolving (Bressan, Chiosi & Fagotto 1994), with $M_R = -22.6$ for RLQs and $M_R = -21.8$ for RQQs at $z \sim 0$ (see for example Kotilainen et al. 2006), we give a first order estimate of the galaxy component flux in the 8 SLOAN & 2MASS filters. An object is excluded from the sample if the estimated flux of the host galaxy is greater than 20% of the observed flux. The excluded objects (~ 1000) are mostly weak, nearby ($z < 0.5$) quasars. We also tested if the removal of quasars with substantial host galaxies could be done by looking at the difference between PSF and model magnitudes in SDSS. The results reported in the following remain substantially unchanged.

2.5 Final sample

The final sample (see Table 1, available in complete form electronically) consists of 887 QSOs, of which 774 RQQs and 113 RLQs.

Figures 1 and 2 show the magnitude and redshift distributions of the radio loud and radio quiet subsamples, indicating a substantial difference between the two classes. This behaviour is well known and it is usually attributed to the cosmological evolution of quasar radio properties or to a different density evolution for RLQs and RQQs (e.g. White et al. 2007; Jiang et al. 2007). The issue is obviously relevant to our discussion and it is considered in section 3.

¹ Equation (1) should be applied to rest-frame data, but this correction requires the assumption of a spectral shape of the objects. Here we choose to evaluate this ratio based on observed data; we verified that the difference is completely negligible.

² We verified that this limit on the separation angle causes the omission of about 20% objects which belong to both catalogues, but drastically reduces the probability of mismatch in the selection of the objects.

Table 1. The final sample. Monochromatic fluxes are derived from SDSS (col. 4–8), 2MASS (col. 9–11) and FIRST (col. 12) and corrected for Galactic extinction; units are 10^{-4} Jy. In col. (12), “n.d.” means “not detected”. The complete version of this table is available in electronic form.

α (J2000)	δ (J2000)	z	SDSS					2MASS			FIRST	R_{r-o}
			F_u	F_g	F_r	F_i	F_z	F_J	F_H	F_K	$F_{20\text{cm}}$	
(1)	(2)	(3)	(4)	(5)	(6)	(7)	(8)	(9)	(10)	(11)	(12)	(13)
00 01 10.97	-10 52 47.5	0.528	2.69	3.40	3.21	3.53	3.24	3.38	4.82	6.46	n.d.	< 10
00 14 20.37	-09 18 49.4	1.083	2.01	2.82	4.25	3.95	3.97	5.26	4.12	6.80	57.3	19.6
00 18 55.22	-09 13 51.2	0.756	2.86	4.25	5.09	5.12	5.62	5.88	6.07	7.12	n.d.	< 10
00 24 11.66	-00 43 48.1	1.795	1.73	2.08	2.29	2.69	2.57	2.67	3.44	4.88	11.7	5.55
00 29 14.21	-09 00 16.1	2.091	0.71	1.16	1.66	2.02	2.70	3.60	3.46	5.37	n.d.	< 10
00 30 09.40	-09 02 23.1	1.786	2.59	2.51	2.69	3.42	3.41	3.09	5.26	3.25	n.d.	< 10
00 34 13.04	-01 00 26.9	1.292	4.72	5.03	5.64	5.81	5.54	5.08	5.62	6.86	n.d.	< 10
00 36 26.11	-09 00 14.2	0.951	1.86	1.93	2.05	1.89	1.89	2.88	1.83	4.98	n.d.	< 10
00 36 33.93	-10 12 28.8	2.082	1.63	1.89	2.06	2.33	2.68	2.69	2.79	4.05	n.d.	< 10
00 37 14.82	-00 45 54.1	1.020	1.66	1.86	2.12	1.96	2.16	2.48	1.65	3.41	n.d.	< 10
00 38 23.81	-00 00 25.1	1.605	1.63	1.79	2.12	2.52	2.67	3.33	3.12	3.11	n.d.	< 10
00 38 42.66	-09 47 12.8	1.989	3.65	3.97	4.45	4.82	5.29	4.39	3.60	5.18	n.d.	< 10
00 42 22.29	-10 37 43.8	0.424	9.13	11.3	9.75	10.0	12.5	7.87	10.8	17.8	n.d.	< 10
00 46 13.54	+01 04 25.7	2.152	1.51	1.90	2.27	2.70	3.11	4.02	4.41	6.35	30.4	15.6
...

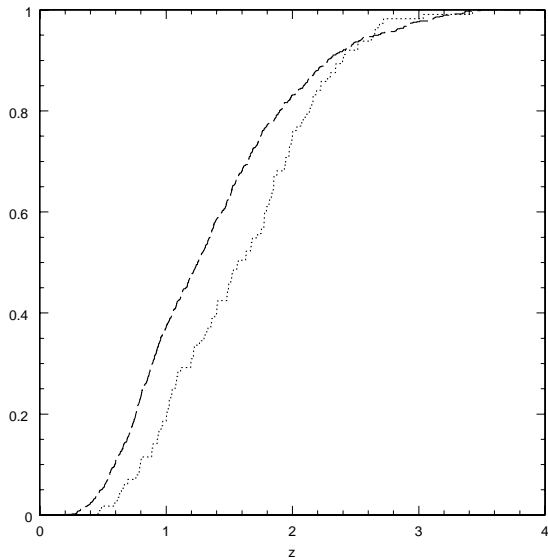


Figure 1. Cumulative redshift distribution of the final sample. Dotted line refers to the RLQ and dashed line to the RQQ.

3 SPECTRAL ENERGY DISTRIBUTIONS (SEDS)

In order to construct and compare the SEDs of RQQs and RLQs, we first evaluated the rest-frame SEDs of single objects. For each one, the SED consists of 8 data-points $\log(\nu)$ – $\log(\nu L_\nu)$, which are linearly interpolated. In order not to be affected by the well known bias which favours more luminous objects at higher redshift, using the standard procedure (e.g. Elvis et al. 1994), the SEDs of the radio loud and radio quiet samples have then been normalized separately at $10^{14.8}$ Hz.

The average SEDs of the two samples have been de-

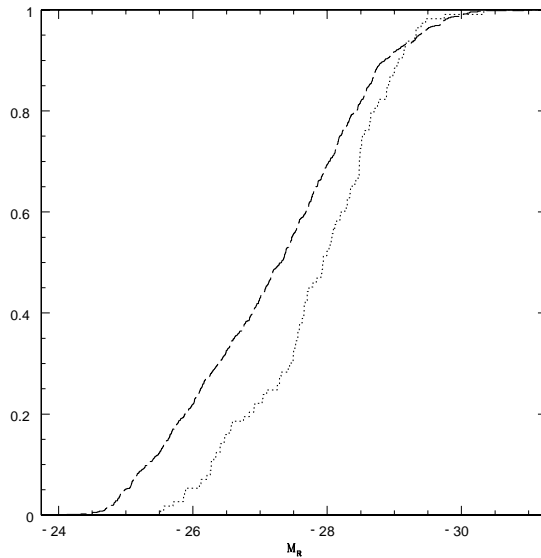


Figure 2. Cumulative M_R distribution of the final sample. Dotted line refers to the RLQ and dashed line to the RQQ.

termined evaluating the average value of $\log(\nu L_\nu)$ at each frequency.

Fig. 3 shows mean SED of the whole sample and those of the RLQ and RQQ subsamples, and in Table 2 we give the number of data-points which contribute to the mean for selected values of $\log(\nu)$, the corresponding average z and the mean value of $\log(\nu L_\nu)$ with corresponding errors. The overall SEDs are similar to those reported by Elvis et al. 1994 and Richards et al. 2006 (see Fig. 4). The strongest feature is the so-called 1 micron inflexion, where the slope of the SED changes sign in a νL_ν vs. ν representation. Here, the optical-ultraviolet continuum rises above the infrared and forms a “UV bump” (e.g. Shields 1978; Malkan & Sargent 1982; Elvis et al. 1994), which is most often interpreted

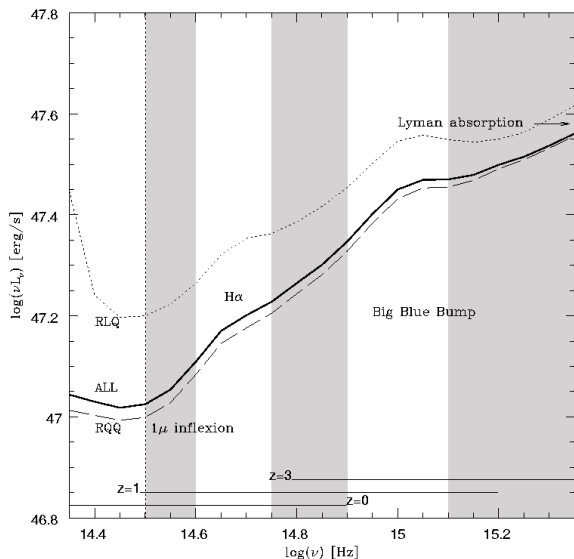


Figure 3. SED for the entire sample of quasar (solid line), RLQs (dotted line) and RQQs (dashed line). The horizontal lines show the spectral region available at different redshifts. The grey regions indicate the spectral ranges where the power law fit is performed.

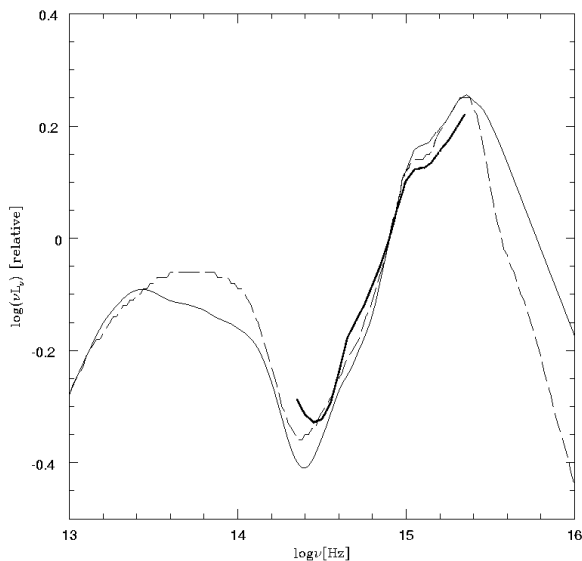


Figure 4. SED for our entire sample of quasar (thick solid line), compared to the SEDs obtained by Elvis et al. 1994 (thin solid line) and by Richards et al. 2006 (thin dashed line). The three SEDs have been normalized at $10^{14.9}$ Hz.

in terms of thermal emission from an accretion disc (e.g., Malkan 1983; Czerny & Elvis 1987).

At high frequencies ($\nu \gtrsim 10^{15.35}$ Hz) the SEDs of all the objects are strongly contaminated by the Lyman α forest; the small bump at $\sim 10^{14.66}$ Hz is due to the presence of the H α large emission line.

It is apparent that RLQs are softer than RQQs. In particular, we compare the slope between the 1 micron inflexion

and the Lyman α forest. The spectral index α (such that $F_\nu \propto \nu^\alpha$) is derived for each object by fitting with a power law the observed fluxes in the spectral range between $10^{14.5}$ and $10^{15.35}$ Hz, excluding the data points affected by the most prominent emission features (i.e. $\sim 10^{14.6} - 10^{14.75}$ Hz, $10^{14.9} - 10^{15.1}$ Hz).

Table 3 reports the mean values of α , the standard deviation and the error on the mean value for the RL and RQ subsamples and Figure 5 shows the cumulative distribution of the spectral index for the two populations. The slopes of the RLQs and the RQQs are statistically different at more than 99% confidence level, with RLQs being softer. The spectral indices of the two populations in the optical region differ by ~ 0.2 , with $\alpha = -0.55 \pm 0.41$ (± 0.04) for RLQs and $\alpha = -0.31 \pm 0.32$ (± 0.01) for RQQs (where the uncertainties are the standard deviations and the errors on the mean respectively). A Kolmogorov-Smirnov test indicates that the probability of RLQs and RQQs to be drawn from the same underlying population is negligible ($P \sim 10^{-7}$). This is a strong indication that the two populations are intrinsically different, in the sense that radio loud objects are systematically redder than radio quiet quasars.

In Section 2.3 we noted that the request of a 2MASS detection introduces a bias in the sample, as among high redshift (low luminosity) objects the redder ones are more likely detected. Consequently, the blue side of the resulting SEDs (which is dominated by high redshift objects) are slightly softer with respect to the SED of an unbiased sample. This effect can be quantified by constructing the mean SEDs on the whole SLOAN sample, i.e. without the request of a 2MASS detection. The shape of the SEDs is modified as expected by the bias introduced, but it is noticeable that the difference between the SEDs of RLQs and RQQs (which is our main result) remains substantially unchanged if we consider the whole SLOAN sample to construct the SED for $\log(\nu) > 14.8$ (where the 2MASS data are unimportant) and the SLOAN-2MASS sample to construct the SED for $\log(\nu) < 14.8$ (where the introduced bias is negligible). The average spectral indices of the RL and RQ populations, as determined on these SEDs, are respectively $\alpha = -0.40$ and $\alpha = -0.22$, with again $\Delta\alpha \sim 0.2$.

Since we are interested in the study of the shape of the SED with reference to the radio power, independently of any other parameter, we now construct a number of RQQ samples matched in absolute magnitude to the RLQs³. We verify that the RQQ matched samples automatically result well matched to the RLQs also in redshift.

Table 3 reports the average results of 10 random matched samples. The SEDs of the RQQ matched samples are on average slightly softer than those of the entire RQQ population ($\Delta\alpha = 0.05$), however the Kolmogorov-Smirnov test indicates that the probability of RLQs and all the RQQ matched samples to be drawn from the same underlying population is still negligible ($P \sim 10^{-3}$; the value is greater than before as the sample has been drastically reduced), and the difference of the mean spectral indices is again ~ 0.2 . This is consistent with the fact that the whole RQQ population and

³ An RQQ with a given luminosity L is extracted from the RQQ population with probability proportional to the luminosity density of the RLQs.

Table 2. For selected frequencies, we report the number of data-points which contribute to the SED of RLQs and RQQs, the mean redshift and its standard deviation, the luminosity, its standard deviation and the error on the mean. The luminosities are normalized at $\log(\nu L_\nu(10^{14.8}\text{Hz}))$.

RLQ				RQQ		
$\log(\nu)$ [Hz]	Num.	z	$\log(\nu L_\nu)$ [erg s $^{-1}$]	Num.	z	$\log(\nu L_\nu)$ [erg s $^{-1}$]
14.35	3	0.514 ± 0.070	$47.446 \pm 0.292(\pm 0.207)$	87	0.481 ± 0.098	$47.013 \pm 0.132(\pm 0.014)$
14.40	13	0.671 ± 0.115	$47.241 \pm 0.163(\pm 0.047)$	190	0.613 ± 0.145	$47.003 \pm 0.123(\pm 0.009)$
14.45	26	0.815 ± 0.171	$47.197 \pm 0.172(\pm 0.034)$	301	0.725 ± 0.190	$46.993 \pm 0.117(\pm 0.007)$
14.50	39	0.924 ± 0.213	$47.200 \pm 0.145(\pm 0.023)$	398	0.829 ± 0.250	$46.999 \pm 0.105(\pm 0.005)$
14.55	55	1.069 ± 0.293	$47.223 \pm 0.131(\pm 0.018)$	513	0.961 ± 0.331	$47.028 \pm 0.102(\pm 0.004)$
14.60	76	1.256 ± 0.396	$47.264 \pm 0.115(\pm 0.013)$	609	1.077 ± 0.407	$47.084 \pm 0.097(\pm 0.004)$
14.65	95	1.412 ± 0.475	$47.321 \pm 0.091(\pm 0.009)$	686	1.184 ± 0.489	$47.145 \pm 0.089(\pm 0.003)$
14.70	106	1.511 ± 0.536	$47.353 \pm 0.072(\pm 0.007)$	733	1.261 ± 0.559	$47.176 \pm 0.074(\pm 0.003)$
14.75	112	1.576 ± 0.591	$47.363 \pm 0.040(\pm 0.004)$	757	1.311 ± 0.615	$47.205 \pm 0.039(\pm 0.001)$
14.80	113	1.592 ± 0.613	$47.386 \pm 0.000(\pm 0.000)$	774	1.353 ± 0.671	$47.244 \pm 0.000(\pm 0.000)$
14.85	113	1.592 ± 0.613	$47.417 \pm 0.036(\pm 0.003)$	774	1.353 ± 0.671	$47.281 \pm 0.030(\pm 0.001)$
14.90	113	1.592 ± 0.613	$47.454 \pm 0.067(\pm 0.006)$	774	1.353 ± 0.671	$47.328 \pm 0.051(\pm 0.002)$
14.95	113	1.592 ± 0.613	$47.502 \pm 0.090(\pm 0.008)$	774	1.353 ± 0.671	$47.384 \pm 0.064(\pm 0.002)$
15.00	113	1.592 ± 0.613	$47.546 \pm 0.108(\pm 0.010)$	772	1.356 ± 0.669	$47.432 \pm 0.077(\pm 0.003)$
15.05	113	1.592 ± 0.613	$47.558 \pm 0.119(\pm 0.011)$	752	1.383 ± 0.657	$47.453 \pm 0.087(\pm 0.003)$
15.10	110	1.622 ± 0.595	$47.549 \pm 0.131(\pm 0.013)$	695	1.454 ± 0.633	$47.455 \pm 0.097(\pm 0.004)$
15.15	103	1.685 ± 0.560	$47.544 \pm 0.150(\pm 0.015)$	599	1.574 ± 0.600	$47.468 \pm 0.110(\pm 0.005)$
15.20	90	1.798 ± 0.507	$47.550 \pm 0.179(\pm 0.019)$	481	1.741 ± 0.553	$47.491 \pm 0.128(\pm 0.006)$
15.25	75	1.935 ± 0.439	$47.563 \pm 0.207(\pm 0.024)$	386	1.891 ± 0.515	$47.509 \pm 0.134(\pm 0.007)$
15.30	59	2.079 ± 0.381	$47.589 \pm 0.207(\pm 0.027)$	269	2.108 ± 0.472	$47.532 \pm 0.157(\pm 0.010)$
15.35	41	2.241 ± 0.345	$47.616 \pm 0.189(\pm 0.030)$	173	2.350 ± 0.422	$47.556 \pm 0.149(\pm 0.011)$

Table 3. Mean values of the spectral index α in the optical–UV region, standard deviation and error on the mean, for the RL and RQ subsamples. Col. 6 reports the Kolmogorov-Smirnov probability that the RLQs and the RQQs (or RQQ matched sample) are drawn from the same population.

Samples (1)	# RLQ (2)	α_{RLQ} (3)	# RQQ (4)	α_{RQQ} (5)	P_{KS} (6)
Total sample	113	$-0.55 \pm 0.41(\pm 0.04)$	774	$-0.31 \pm 0.32(\pm 0.01)$	10^{-7}
Matched samples	"	"	112	$-0.36 \pm 0.29(\pm 0.03)$	10^{-3}
$z < 0.8$	12	$-0.64 \pm 0.55(\pm 0.16)$	181	$-0.21 \pm 0.37(\pm 0.03)$	10^{-2}
$0.8 < z < 1.2$	23	$-0.41 \pm 0.34(\pm 0.07)$	188	$-0.26 \pm 0.31(\pm 0.02)$	10^{-1}
$1.2 < z < 1.6$	22	$-0.66 \pm 0.50(\pm 0.11)$	157	$-0.34 \pm 0.30(\pm 0.02)$	10^{-4}
$1.6 < z < 2.0$	28	$-0.56 \pm 0.40(\pm 0.08)$	117	$-0.37 \pm 0.27(\pm 0.03)$	10^{-2}
$z > 2.0$	28	$-0.51 \pm 0.34(\pm 0.07)$	131	$-0.42 \pm 0.28(\pm 0.02)$	10^{-1}

an RQQ matched sample have identical distributions in α ($P \sim 90\%$) and it is a strong indication that the radio loud and radio quiet populations are intrinsically different, in the sense that radio loud objects are systematically redder than radio quiet quasars independently of the average luminosity or cosmic time.

Finally we compare RLQs and RQQs in different redshift bins (see again Table 3), and this test shows that the color difference between the RL and RQ populations is apparent in all the redshift ranges.

4 SUMMARY AND DISCUSSION

The aim of the present paper is the study of the continuum emission in the NIR to UV region of a quasar sample, in order to compare and contrast the SEDs of the RLQ and

RQQ subsamples. We selected a sample of quasars with both SLOAN and 2MASS detection, to study a spectral range from the NIR (for low- z objects) to the UV (for high- z QSOs). The sample consists of 887 objects, of which 113 RLQs and 774 RQQs.

For each subsample we constructed the mean SED and evaluated the average spectral index in the NIR to UV region. The slope of the underlying power-laws is significantly different: the spectral indices of the two population are statistically different at more than 99% confidence, both for the whole sample and dividing the sample in redshift bins. The difference is present also considering samples well matched in absolute magnitude and redshift.

If the blue bump is due to the superposition of black body emissions from an accretion disc, then the color difference between RLQs and RQQs should be interpreted in

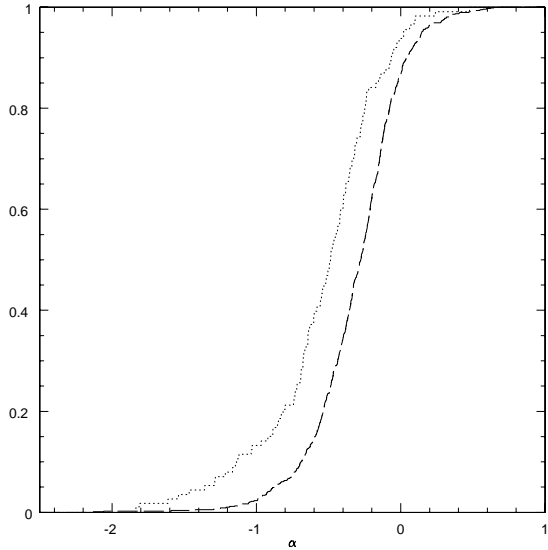


Figure 5. Cumulative distribution of the spectral index for the RL (dotted line) and RQ (dashed line) subsamples.

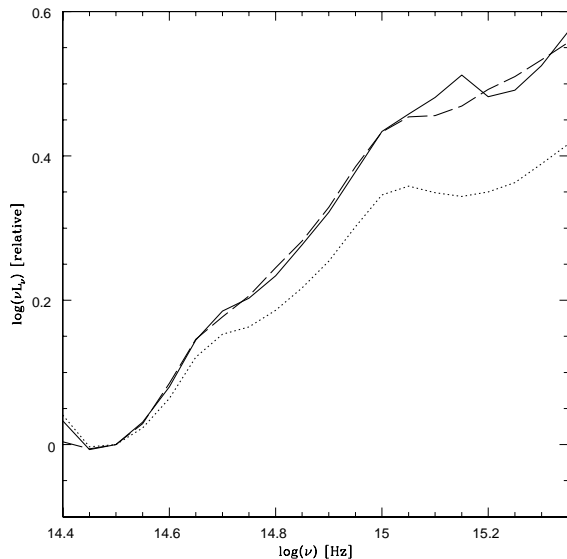


Figure 6. Comparison of the SED of RQs (dashed line) to the SED of RLs (dotted line). When RLs are corrected for an additional dust extinction ($\Delta A_V = 0.16\text{mag}$, solid line), no difference is apparent.

terms of different mean temperatures, in the sense that RQs are hotter.

We first examine the possibility that the difference in the SEDs of RLs and RQs is due to an enhanced dust extinction in radio loud objects, as it has been suggested e.g. by Francis et al. (2000). In Fig. 6 we compare the SED of RQs to the SED of RLs, when RLs are additionally corrected for dust extinction with respect to RQs: the offset between the SEDs of the two population is minimized adopting $\Delta A_V = 0.16\text{mag}$. The differences are now com-

pletely negligible, supporting the hypothesis that RL objects are more subject to dust extinction than RQs. The problem would be reconducted to understand why RLs are more extinguished than RQs. *A priori* this could be related to a difference in the inclination angle distribution. Alternatively, it could be that the conditions of dust production are related to those justifying large radio emission.

We then focus on the possibility that the difference of disc temperature of RLs and RQs is real. Since the temperature of the inner disc scales as $M_{\text{BH}}^{-0.25}$ (e.g. Shakura & Sunyaev 1973), the difference may be attributed to the fact that the black holes of radio loud quasars are supposedly more massive (e.g. Dunlop et al. 2003; Falomo et al. 2004; Labita et al. 2007).

The color difference may be linked to the BH spin (Stawarz, Sikora & Lasota 2007), as radio emission is usually ascribed to a faster spinning. However, spinning BHs are expected to have a shorter last stable orbit radius, and then a hotter disc, inconsistently with our results.

Obviously it is possible that the non-thermal (power law) continua of RLs and RQs are intrinsically different. Supposing that the non-thermal component accounts for 80% at $10^{14.5}\text{Hz}$, while at $10^{15.35}\text{Hz}$ (in the Big Blue Bump) the thermal component is dominant and accounts for 80%, our data are consistent with a picture where the underlying power-laws of RLs and RQs have $\alpha_{\text{RLQ}} = -1.2$ and $\alpha_{\text{RQ}} = -1.0$ respectively, whereas the thermal bumps are indistinguishable. The problem would be reconducted to understand why the non-thermal continuum of RLs is softer than RQs. It has been suggested (i.e. Francis et al. 2000) that in radio loud samples there is a significant chance of synchrotron contamination of the rest-frame R-band nuclear luminosities, due to the presence of the relativistic jets. This effect explains the red color of QSOs in high-frequency selected radio samples (i.e. the PKS survey, e.g. Francis et al. 2001), that suffer from a bias towards pole-on radio sources which are relativistically boosted above the survey flux limit, but no obvious explanation can be invoked to justify the color difference in our sample.

ACKNOWLEDGEMENTS

We are grateful to Dr. M. Strauss for constructive criticism, and to Dr. D. Bettoni for help in the use of SLOAN archives. This work was partially supported by PRIN 2005/32.

REFERENCES

- Barkhouse W.A., Hall P.B., 2001, AJ, 121, 284
- Becker R.H., Helfand D.J., White R.L., Gregg M.D., Laurent-Muehleisen S.A., 2003, VizieR On-line Data Catalog, VIII/71
- Bressan A., Chiosi C., Fagotto F., 1994, ApJS, 94, 63
- Cutri R.M. et al., 2003, VizieR On-line Data Catalog, II/246
- Czerny B., Elvis M., 1897, ApJ, 321, 305
- Dunlop J.S., McLure R.J., Kukula M.J., Baum S.A., O’Dea C.P., Hughes D.H., 2003, MNRAS, 340, 1095
- Falomo R., Kotilainen J.K., Pagani C., Scarpa R., Treves A., 2004, ApJ, 604, 495
- Elvis M. et al., 1994, ApJS, 95, 1
- Francis P.J., Hewett P.C., Foltz C.B., Chae F.H., Weymann R.J., Morris S.L., 1991, ApJ, 373, 465
- Francis P.J., Whiyng M.T., Webster R.L., 2000, PASA, 53, 56

- Francis P.J., Drake C.L., Whiting M.T., Drinkwater M.J., Webster R.L., 2001, PASA, 18, 221
Goldshmidt P., Kukula M.J., Miller L., Dunlop J.S., 1999, ApJ, 511, 612
Goldshmidt P., Kukula M.J., Miller L., Dunlop J.S., 1999, ApJ, 511, 612
Hooper E.J., Impey C.D., Foltz C.B., 1997, ApJL, 480, 95
Ivezić Z. et al. 2002, AJ, 124, 2364
Jiang L., Fan X., Ivezić Z., Richards G.T., Schneider D.P., Strauss M.A., Kelly B.C., 2007, ApJ, 656, 680
Kellermann K.I., Sramek R., Schmidt M., Shaffer D.B., Green R., 1989, AJ, 98, 1195
Kotilainen J.K., Falomo R., Labita M., Treves A., Uslenghi M., 2007, 660, 1039
Labita M., Falomo R., Treves A., 2006, MNRAS, 373, 551
Malkan M.A., Sargent W.L.W., 1982, ApJ, 254, 22
Malkan M.A., 1983, ApJ, 268, 582
Mannucci F., Basile F., Poggianti B.M., Cimatti A., Daddi E., Pozzetti L., Vanzi L., 2001, MNRAS, 326, 745
Richards G.T. et al., 2006, ApJS, 166, 470
Sanders D.B., Phinney E.S., Neugebauer G., Soifer B.T., Matthews K., 1989, ApJ, 347, 29
Schneider et al., 2005, AJ, 130, 367, VizieR On-line Data Catalog, VII/243
Shakura N.I., Sunyaev R.A., 1973, A&A, 24, 337
Shields G.A., 1978, Nature, 272, 706
Stawarz L., Sikora M., Lasota J.P., 2007, to appear in ASP Conference Series (astro-ph/0707.2368)
White R.L., Helfand D.J., Becker R.H., Glickman E., de Vries W., 2007, ApJ, 654, 99